Valence photoionization and resonant Auger decay of Sb_4 clusters at resonances below the 4*d* ionization threshold

S. Urpelainen,[1,*] J. Niskanen,[2] J. A. Kettunen,[2] M. Huttula,[2] and H. Aksela[2]
[1]*MAX-lab, Lund University, P.O. Box 118, SE-221 00 Lund, Sweden*
[2]*Department of Physics, University of Oulu, P.O. Box 3000, FIN-90014 Oulu, Finland*
(Received 9 December 2010; published 28 January 2011)

The valence photoionization and resonant Auger decay at 4*d* resonances below the 4*d* ionization threshold in Sb_4 clusters have been studied experimentally by means of photoelectron spectroscopy. The 4*d* absorption spectrum in the photon energy region from 30 to 36 eV has been recorded using the constant ionic state (CIS) partial electron yield (PEY), and the CIS spectra for various ionic states are presented. The photoelectron spectra at various resonant positions are recorded, and the results and their interpretation are presented. The findings provide experimental proof of the previous assignment of the various structures of the inner valence photoelectron spectrum.

DOI: 10.1103/PhysRevA.83.015201 PACS number(s): 36.40.Mr, 36.20.Kd, 32.80.Fb

I. INTRODUCTION

A large emphasis is presently put on both experimental and theoretical studies of clusters formed of atoms or molecules. At the moment an especially hot topic is studying the highly size-dependent bulk properties, such as electric conductivity and magnetism, of various size metal clusters. Thus it is necessary not only to obtain experimental and theoretical information about clusters available using present techniques, but to develop novel methods for creating clusters of specific sizes as well. For example, in experimental studies of neutral unsupported metal clusters, the techniques for cluster production—such as the pick-up or exchange metal cluster technique [1,2]—create a wide distribution of various cluster sizes. The signal from the directly evaporated parent species is abundant in the recorded spectra as well, when using these methods. Thus it is extremely important to know the various spectral features arising from the parent species not only for the fundamental physical information contained in them, but also in order to be able to remove the parent species' contribution from the spectra to have as pure a signal as possible from the larger clusters.

Antimony (Sb) together with its various compounds is a commonly used material in various industrial processes, especially in the production of semiconductor devices. For cluster studies, Sb is an ideal target as it evaporates readily as tiny clusters at low temperatures [3], predominantly as Sb_4 clusters. To be able to understand the electronic structure and dynamics of larger clusters, the properties of their building blocks from elemental atoms to clusters made of a few to some tens of atoms need to be well known. This is especially true, when studying the evolution of band formation as a function of cluster size, as an addition of only a few atoms to the cluster can drastically change its electronic properties. The Sb_4 received notable attention in the 1980s and 1990s, when the valence shells of the Sb, Sb_2, Sb_4, and Sb_8 clusters were probed using He I photoelectron spectroscopy [4–9]. In addition, a study of the $4d \rightarrow \epsilon f$ shape resonance of various sized Sb clusters in the energy range 20–120 eV was performed [10]. More detailed studies of the inner valence region of the photoelectron spectrum have, however, to the best of our knowledge not been performed.

In the present study we have continued our earlier work on the photoionization of Sb_4 clusters [11–13], where the fragmentation of the Sb_4 clusters following 4*d* core ionization and outer and inner valence ionization was studied using the photoelectron-ion and photoelectron-ion-ion coincidence techniques; the 4*s* and 4*p* photoionizations were studied using photoelectron spectroscopy. In the earlier work, the wide bands appearing in the valence photoelectron spectra at electron binding energies between 11 and 20 eV were assigned as a combination of correlated $c_1|5t_2^{-1}\rangle + c_2|(5a_1 6t_2 2e)^{-2} n'l'\rangle$ states and shake-up satellites accompanying the $(5a_1 6t_2 2e)^{-1}$ ionization based on molecular calculations, bonding properties of the orbitals, and the fragmentation products observed in coincidence with the photoelectrons. The notation *nl* in this work is used to identify states occupied in direct photoionization accompanied by a shake-up transition and $n'l'$ to distinguish the states occupied through electron correlation effects (correlation satellites). In this work we present the absorption spectrum of Sb_4 clusters just below the 4*d* ionization threshold recorded using the constant ionic state (CIS) method together with electron spectra recorded at photon energies corresponding to $4d \rightarrow v$ resonances, where the *v* denotes virtual orbitals not occupied in the ground state such as the lowest unoccupied molecular orbital (LUMO) or the *nl* and $n'l'$ Rydberg states. The energy region was extended to cover binding energies up to 26 eV.

II. EXPERIMENTS

The experiments were performed on the FINEST beamline branch on the I3 beamline of the 700-MeV MAX-III electron storage ring at MAX-laboratory (Lund, Sweden). A detailed description of the FINEST branch line and the I3 beamline can be found in Refs. [14–16]. In short, the beamline is sourced by an APPLE-II type elliptically polarizing undulator (EPU) and the radiation is monochromatized using a 6.65-m off-axis Eagle type monochromator for ultrahigh resolution photon energy selection. The FINEST branch consists of an Au coated

*samuli.urpelainen@maxlab.lu.se

toroidal refocusing mirror and a highly efficient differential pumping setup allowing high pressure and vapor phase studies without the risk of contaminating the beamline optics.

For recording the CIS spectra and the electron spectra a modified Scienta SES-100 hemispherical electron energy analyzer was employed [17,18]. The pass energy of the analyzer was set to 100 eV corresponding to an electron energy window width of approximately 11 eV, and the photon energy was scanned while recording electrons with a constant binding energy at each photon energy step. The entrance slit of the analyzer was chosen to be 0.8 mm (curved) corresponding to analyzer broadening of 400 meV. The monochromator entrance and exit slit were both set to 950 μm as the inherent width of the resonant lines was nearly 1 eV and the photon energy bandwidth was approximated to be in the order of 10 meV. The valence and inner valence photoelectron spectra were then recorded off-resonance, on the resonances, and between the two distinct resonances. The spectra were recorded with analyzer pass energy of 20 eV and entrance slit of 0.8 mm (curved). All experiments were performed using vertically linearly polarized radiation from the undulator, and the electron detection angle was set to the magic angle of 54.7° with respect to the electric field vector of the incoming light so that the measured photoelectron intensities are directly proportional to the ionization cross section.

The Sb vapor was produced using an inductively heated oven [19] and the Sb powder was placed inside a stainless steel crucible with a single hole for vapor beam output. The efficient induction heating allowed quick bake-out of the crucible reducing the amount of the most common residual gases and vapors such as H_2O, CO_2, and CO to a negligible level. This made it possible to record pure Sb spectra, as the valence photoelectron lines of these compounds would otherwise overlap heavily with the lines produced by inner valence ionization of Sb_4.

As the photoelectron spectra were recorded over a wide range of kinetic energies, the transmission of the electron analyzer was determined by recording the He 1s photoelectron line throughout the kinetic energy region of the photoelectron spectra at the same analyzer settings. The used transmission correction procedure is described in detail in Ref. [20]. The CIS spectra were normalized with the current measured on an AXUV-100 photodiode corrected with the quantum efficiency at the given photon energy [21].

III. RESULTS AND DISCUSSION

The recorded CIS spectrum is presented in Fig. 1. The arrows A–D denote the photon energies (32 eV, 33.27 eV, 33.83 eV, and 34.43 eV, respectively) at which the photoelectron spectra presented in Fig. 2 were recorded. Figure 1 shows the resonances assigned to $4d \rightarrow v$ type transitions. The photon energies on resonances were chosen to correspond to the maxima of the $5a_1$ photoline (B and D). The CIS spectrum consists of clearly more than the two spin-orbit split lines that would arise from excitations from the $4d_{3/2}$ and $4d_{5/2}$ subshells. As the 4d electrons can occupy some 20 orbitals and the coupling of the 4d hole to the electron on the v state—which is further split by the spin-orbit effect and possibly the Jahn-Teller effect [22]—yields in a multitude of

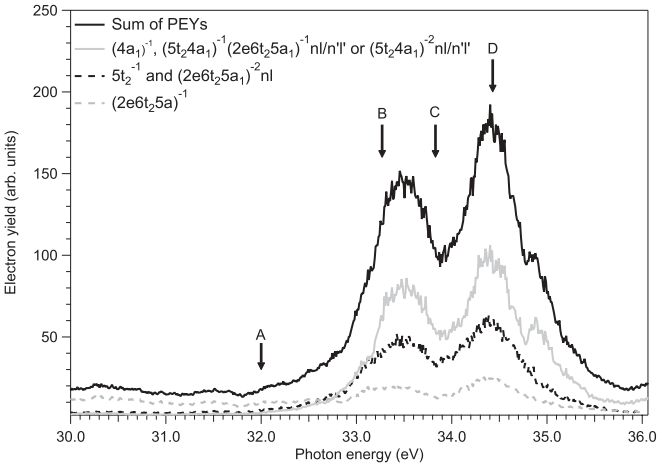

FIG. 1. CIS spectra recorded monitoring the valence and inner valence region of the Sb_4 photoelectron spectrum. The black solid line denotes the sum of all PEY spectra, the dashed black line the inner valence $5t_2^{-1}$ and $(2e6t_25a_1)^{-2}nl$ shake-up PEY, the dashed gray line the outer valence $(2e6t_25a_1)^{-1}$ PEY, and the gray solid line the inner valence $4a_1^{-1}$, $(5t_24a_1)^{-1}(2e6t_25a_1)^{-1}n'l'$ PEY, and possible $(5t_24a_1)^{-2}n'l'$ PEY. The arrows (labeled A–D) show the photon energies, where detailed photoelectron spectra were recorded.

available states and thus spectral features, no clear assignment of the absorption spectrum features could be made without careful theoretical calculations. Such calculations were out of the scope of this report.

At the nonresonant position A the electron spectrum (A in Fig. 2) resembles that reported in Ref. [12]. The only difference is the much lower relative intensity of the inner valence $5t_2$ and satellite region with respect to the outer valence region and the relative intensities of the lines. This can be explained by the fact that the energy is now well below the $4d \rightarrow \epsilon f$ shape resonance. The spectra recorded at the resonances (B and D in Fig. 2) and between the resonances (33.83 eV, a mixture of the two resonances, C in Fig. 2) show significant enhancement in the intensities of the lines in the $5t_2$ and satellite region. This behavior is expected as the resonant excitation lifts one electron from the core 4d orbital to the LUMO or a higher lying Rydberg orbital in the intermediate state. These excited states can then decay via two different processes: a participator or a spectator Auger process. In the participator Auger process the core hole is filled by an electron from the valence orbitals and the excited electron is ejected out of the system leaving the target in the same ionic state as in the direct photoionization process. The spectator Auger process leaves the system in an excited state so that the core hole is filled by an electron on one of the valence orbitals and another valence electron is ejected away from the system. These ionic states correspond energetically to direct photoionization accompanied by a shake-up transition or correlation satellites.

An important difference with respect to the spectrum presented in Ref. [12] is that the structures start at notably lower binding energies than the 12 eV reported in Ref. [12] at around 11 eV or even 9.5 eV overlapping with the $5a_1$ photoline. These structures are weak even at the resonant photon energies and thus it is not surprising that they were

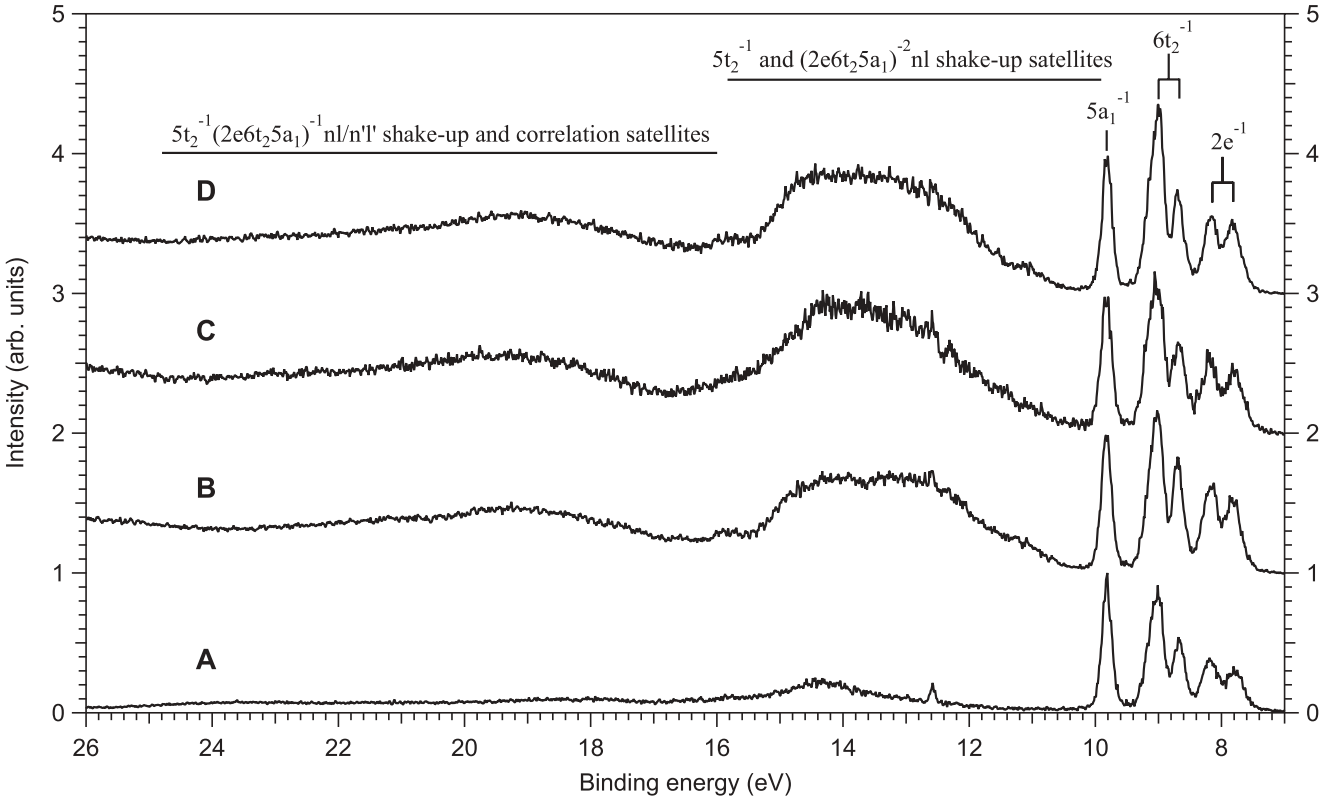

FIG. 2. Valence and inner valence photoelectron spectra recorded at photon energies 32 eV (A), 33.27 eV (B), 33.83 eV (C), and 34.43 eV (D). The spectra recorded on and between the resonances show significant enhancement of intensity for the inner valence and satellite lines.

not observed in earlier studies. As these energies are much lower than the theoretically predicted binding energy of the $5t_2$ orbital, it is reasonable to conclude that these states must be the first in the series of shake-up transitions accompanying the $(5a_16t_22e)^{-1}$ ionization supporting the earlier conclusions.

Figure 2 also shows that the spectra recorded at the resonant positions B and D do not significantly differ from each other. Even the spectrum recorded between the two resonances at position C differs from spectra B and D only in slightly weaker intensity in the satellite region. This strongly suggests that both resonances initially populate the same intermediate excited states. In addition, a broad background-like structure can be seen extending from binding energy of approximately 17 eV upward. As this background is not emphasized in the earlier study [12] or in the spectrum A recorded off-resonance it is concluded that the electrons in this region originate from the states corresponding to $5t_2$ ionization accompanied by a shake-up transition to the LUMO or to the correlation satellites. This structure is very similar to the shake-up structure from the $(5a_16t_22e)^{-1}$ ionization, which starts with a small band at around 11.2 eV and continues with a broader band up to 17 eV.

A more careful look at the spectra recorded at the resonant positions reveals that the relative enhancement of the main lines originating from $(5a_16t_22e)^{-1}$ ionization is not as strong as that of the various satellite structures. This is expected as the core-excited states prefer to decay via spectator Auger process as opposed to participator Auger (see, e.g., [23] and references therein), and we can conclude that this must be true also for the direct $5t_2^{-1}$ ionization. This means that most of the intensity in the 10- to 16-eV energy region is due to the $(5a_16t_22e)^{-1}nl$ states. This supports the conclusion made in Ref. [12], which states that the broad intense band centered around 14.32 eV corresponds to the direct $5t_2^{-1}$ photoionization and is not a part of the $(5a_16t_22e)^{-1}$ shake-up satellite structure although they overlap significantly. Figure 2 shows also the onset of another broad structure at approximately 25 eV. This structure could originate from $4a_1^{-1}$ or $(4a_1)^{-1}(5a_16t_22e)^{-1}nl'$ type states as the ionization potential of the $4a_1$ MO is predicted to be at around 22.52 eV [12].

IV. CONCLUSIONS

In this report we have presented the detailed experimental $4d \rightarrow nl$ absorption spectrum recorded using the CIS PEY technique as well as photoelectron and resonant Auger spectra at the various resonant positions. We have provided experimental proof supporting the tentative assignment for the inner valence region of the photoelectron spectrum made in Ref. [12] and have shown that the rich structures in the inner valence region of the photoelectron spectrum can be assigned to various shake-up and correlation satellites.

ACKNOWLEDGMENTS

This work has been financially supported by the Research Council for Natural Sciences of the Academy of Finland and the European Community Research Infrastructure Action under the FP6 "Structuring the European Research Area"

Program (through the Integrated Infrastructure Initiative "Integrating Activity on Synchrotron and Free Electron Laser Sciences"). S.U. acknowledges the Research Council for Natural Sciences and Engineering of the Academy of Finland (Grant No. 135871) and Lund's University for financial support. We thank Minna Patanen for useful conversations and Sergey Osmekhin, Denys Iablonskyi, and the staff of MAX-lab for their assistance during the experiments.

[1] J. Tiggesbäumker and F. Stienkemeier, Phys. Chem. Chem. Phys. **9**, 4748 (2007).
[2] M. Huttula, M.-H. Mikkelä, M. Tchaplyguine, and O. Björneholm, J. Electron Spectrosc. Relat. Phenom. **181**, 145 (2010).
[3] K. Sattler, J. Mühlbach, and E. Recknagel, Phys. Rev. Lett. **45**, 821 (1980).
[4] S. Elbel, J. Kudnig, M. Grodzicki, and H. J. Lempka, Chem. Phys. Lett. **109**, 312 (1984).
[5] L. S. Wang, Y. T. Lee, D. A. Shirley, K. Balasubramanian, and P. Feng, J. Chem. Phys. **93**, 6310 (1990).
[6] L. S. Wang, B. Niu, Y. T. Lee, D. A. Shirley, E. Ghelichkhani, and E. R. Grant, J. Chem. Phys. **93**, 6318 (1990).
[7] L. S. Wang, B. Niu, Y. T. Lee, D. A. Shirley, E. Ghelichkhani, and E. R. Grant, J. Chem. Phys. **93**, 6327 (1990).
[8] V. Kumar, Phys. Rev. B **48**, 8470 (1993).
[9] J. M. Dyke, A. Morris, and J. C. H. Stevens, Chem. Phys. **102**, 29 (1986).
[10] C. Bréchignac, M. Broyer, P. Cahuzac, M. de Frutos, Ph. Labastie, and J.-Ph. Roux, Phys. Rev. Lett. **67**, 1222 (1991).
[11] S. Urpelainen, A. Caló, L. Partanen, M. Huttula, S. Aksela, H. Aksela, S. Granroth, and E. Kukk, Phys. Rev. A **79**, 023201 (2009).
[12] S. Urpelainen, A. Caló, L. Partanen, M. Huttula, J. Niskanen, E. Kukk, S. Aksela, and H. Aksela, Phys. Rev. A **80**, 043201 (2009).
[13] M. Huttula, S.-M. Huttula, S. Urpelainen, L. Partanen, S. Aksela, and H. Aksela, J. Phys. B: At. Mol. Opt. Phys. **42**, 235002 (2009).
[14] S. Urpelainen, Ph.D. thesis, University of Oulu, 2009.
[15] T. Balasubramanian *et al.*, AIP Conf. Proc. **1234**, 661 (2010).
[16] S. Urpelainen, M. Huttula, T. Balasubramanian, R. Sankari, P. Kovala, E. Kukk, E. Nõmmiste, S. Aksela, R. Nyholm, and H. Aksela, AIP Conf. Proc. **1234**, 411 (2010).
[17] M. Huttula, M. Harkoma, E. Nõmmiste, and S. Aksela, Nucl. Instrum. Methods Phys. Res., Sect. A **467**, 1514 (2001).
[18] M. Huttula, S. Heinäsmäki, H. Aksela, E. Kukk, and S. Aksela, J. Electron Spectrosc. Relat. Phenom. **156**, 270 (2007).
[19] M. Huttula, K. Jänkälä, A. Mäkinen, H. Aksela, and S. Aksela, New J. Phys. **10**, 013009 (2008).
[20] J. Niskanen, S. Urpelainen, S. Aksela, H. Aksela, O. Vahtras, V. Carravetta, and H. Ågren, Phys. Rev. A **81**, 043401 (2010).
[21] [http://www.ird-inc.com].
[22] H. Zhang and K. Balasubramanian, J. Chem. Phys. **97**, 3437 (1992).
[23] H. Aksela, S. Aksela, and N. Kabachnik, in *VUV and Soft X-Ray Photoionization*, edited by U. Becker and D. A. Shirley (Plenum Press, New York, 1996).